PS-wave polarity reversal in angle domain common-image gathers

Daniel Rosales and James Rickett [1]

ABSTRACT

The change in the reflection polarity at normal incidence is a fundamental feature of converted-wave seismology due to the vector nature of the displacement field. The conventional way of dealing with this feature is to reverse the polarity of data recorded at negative offsets. However, this approach fails in presence of complex geology. To solve this problem we propose operating the polarity flip in the angle domain. We show that this method correctly handle the polarity reversal after prestack migration for arbitrarily complex earth models.

INTRODUCTION

An important issue in converted wave seismic processing is how to deal with the polarity reversal that occurs near zero-offset. Conventional methodology (Harrison and Stewart, 1993) involves multiplying the data recorded at negative offsets by -1. However, this approach fails where there is structural complexity and non-constant v_p/v_s ratio (γ).

For P-wave datasets, angle-domain common-image gathers [e.g., de Bruin et al. (1991); Prucha et al. (1999)] decompose reflected seismic energy into components from specific opening angles (θ). Since the PS-wave polarity reversal occurs at normal incidence ($\theta = 0$), the angle-domain common-image gathers provide a natural domain in which to address the polarity reversal problem. Moreover, analyzing angle gathers for converted wave seismic data may lead to: velocity analysis and amplitude versus angle analysis for converted waves.

In this work we present a theoretical discussion of the polarity reversal problem. We image PS-wave data into offset-domain CIGs with a prestack recursive depth migration algorithm. We use the radial-trace transformation introduced by Sava and Fomel (2000) to obtain angle-domain gathers after migration. We reinterpret the opening angle (θ) for the case of converted waves, this leads to a solution of the polarity reversal problem that is valid for any structurally complex media.

[1] **email:** daniel@sep.stanford.edu, james@sep.stanford.edu

THEORY

Polarity flip

The polarity inversion visible at zero-offset in converted wave data (PS) is an intrinsic property of the shear wave displacement (Danbom and Domenico, 1988). In a constant velocity medium, the vector displacement field produces opposite movements in the two geophones at either side of the source (Figure 1). This leads to the polarity flip in the seismic gather.

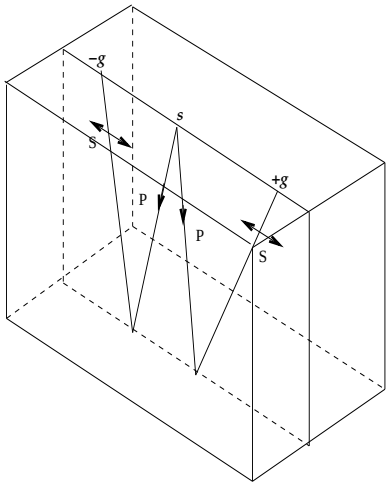

Figure 1: Polarity inversion in converted waves seismic data. `+g` and `-g` correspond to positive and negative polarity in a common shot gather. Modified from Tatham and McCormack (1991). daniel2-pflip [NR]

For media with more complex velocity, the normal incidence ray determines the location of the polarity flip. For flat reflectors in $v(z)$ media, and in areas with constant γ, the normal incidence ray emerges at the surface at zero-offset. However, in general, the P and S-wave ray paths corresponding to the normal-incidence (zero-amplitude) ray will not necessarily emerge at the surface at the same point. Figure 2 illustrates this for the case of a dipping layer and a non-constant γ.

This path deviation produces a polarity reversal at non-zero offset in the data space. In areas of complex structure, the picking of this polarity flip point is difficult; however, in the angle domain (model space), this point is a uniquely determined function of the P-velocity, S-velocity, and reflector dip; therefore, it is easy to correct the polarity flip in the model space.

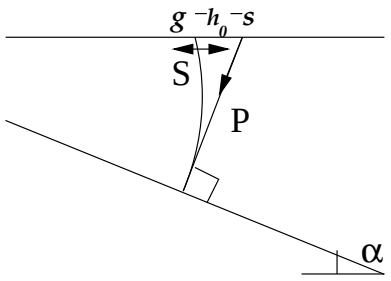

Figure 2: Polarity flip problem for a dipping layer and a non-constant γ. daniel2-pflip2 [NR]

Converted-wave migration by depth extrapolation

Recursive migration methods based on wavefield extrapolation have the advantage over Kirchhoff methods in that they accurately handle the finite-frequency effects of wave-propagation. For example, rough velocity models and triplicating wavefronts that can cause problems for Kirchhoff migrations present no difficulties for recursive methods. Biondi (2000) demonstrated these advantages for a complex 3-D P-wave dataset.

For the examples in this paper, we migrated the prestack data with a shot-profile migration algorithm, imaging the cross-correlation of upgoing and downgoing wavefields at zero-time (Claerbout, 1971); however, the methodology is also applicable for "survey-sinking" shot-geophone algorithms based on the double square root equation (Claerbout, 1985).

Migrating converted waves with conventional wavefield extrapolation algorithms simply involves extrapolating downgoing waves with the P-wave velocity field, and upgoing waves with the S-wave velocity field. The difficulty comes in the interpretation of common-image gathers in terms of incidence angle at the reflector.

Angle domain common image gathers

Both de Bruin et al. (1991) and Prucha et al. (1999) obtain P-wave angle-domain common-image gathers by slant-stacking the wavefields during migration, before invoking the imaging condition. Their methodologies suit shot-profile and shot-geophone algorithms, respectively. However, we follow an alternative approach advocated by Sava and Fomel (2000).

Fomel (1996) presented the following partial differential equation describing an image surface in depth-midpoint-offset space:

$$\tan\theta = -\left.\frac{\partial z}{\partial h}\right|_{t,x}, \tag{1}$$

where θ is the P-wave opening or incidence angle.

For converted waves, θ has a no simple physical interpretation. In this case, θ is a complex function of the P-incidence angle, the S-reflection angle, and the structural dip, α (Figure 3). Figure 3 shows the geometrical relationship between the P-incidence angle, the S-reflection angle, and the structural dip with the opening angle for the converted waves case. Following Fomel's (1996) derivation we will derive the PS relationship for angle domain common image gathers. In order to relate the first-order traveltime derivatives of the PS-wave with the P-incidence angle and the S-reflection angle, we use the well-known equations for apparent slowness

$$\frac{\partial t}{\partial s} = \frac{\sin\alpha_1}{v_p}, \tag{2}$$

$$\frac{\partial t}{\partial r} = \frac{\sin\alpha_2}{v_s}. \tag{3}$$

Considering the traveltime derivative with respect to the depth of the observation surface (z),

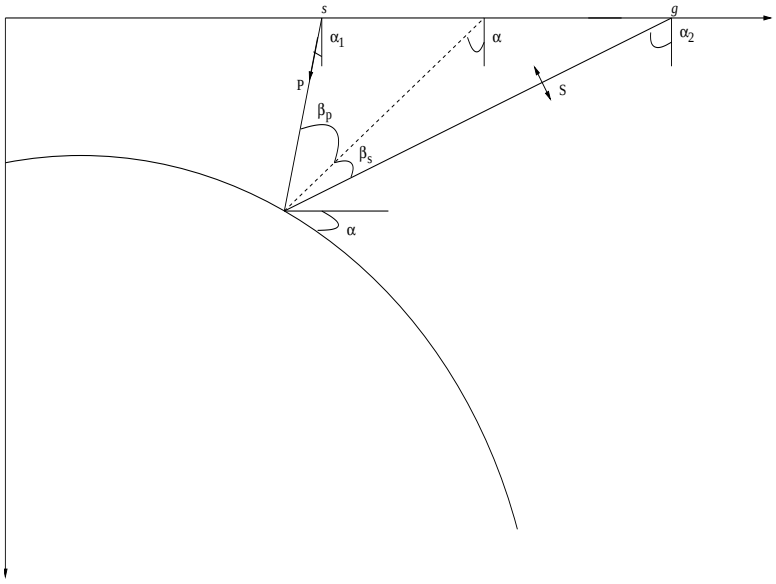

Figure 3: Reflection rays for a PS-data in a constant velocity medium (Adapted from Fomel (1996)). daniel2-sergey [NR]

the contributions of the two branches of the reflected ray add together to form

$$-\frac{\partial t}{\partial z} = \frac{\cos\alpha_1}{v_p} + \frac{\cos\alpha_2}{v_s}. \tag{4}$$

Introducing midpoint $x = \frac{s+r}{2}$ and half-offset $h = \frac{r-s}{2}$ coordinates, and relating α_1 and α_2 with the P-incidence angle (β_p), the S-reflection angle (β_s), and the structural dip (α)

$$\begin{aligned} \alpha_1 &= \alpha - \beta_p, \\ \alpha_2 &= \alpha + \beta_s; \end{aligned}$$

and using the chain rule:

$$\begin{aligned} \frac{\partial t}{\partial x} &= \frac{\partial t}{\partial s} + \frac{\partial t}{\partial r}, \\ \frac{\partial t}{\partial h} &= \frac{\partial t}{\partial r} - \frac{\partial t}{\partial s}. \end{aligned}$$

We can transform relations (2), (3), and (4) to:

$$\frac{\partial t}{\partial x} = \frac{\sin(\alpha-\beta_p)}{v_p} + \frac{\sin(\alpha+\beta_s)}{v_s}, \tag{5}$$

$$\frac{\partial t}{\partial h} = \frac{\sin(\alpha+\beta_s)}{v_s} - \frac{\sin(\alpha-\beta_p)}{v_p}, \tag{6}$$

$$-\frac{\partial t}{\partial z} = \frac{\cos(\alpha-\beta_p)}{v_p} + \frac{\cos(\alpha+\beta_s)}{v_s}. \tag{7}$$

Dividing (6) by (7) and using elementary trigonometric equalities, we obtain:

$$-\frac{\partial z}{\partial h} = \frac{v_p\sin\alpha\cos\beta_s + v_p\sin\beta_s\cos\alpha - v_s\sin\alpha\cos\beta_p + v_s\sin\beta_p\cos\alpha}{v_p\cos\alpha\cos\beta_s - v_p\sin\alpha\sin\beta_s + v_s\cos\alpha\cos\beta_p + v_s\sin\alpha\sin\beta_p} = \tan\theta \tag{8}$$

For $v_p = v_s$, the P-incidence angle will be the same as the S-reflection angle; hence, θ in equation (8) corresponds to the ray incidence angle. However, for converted waves ($v_p \neq v_s$) no such simple physical interpretation exists, and θ relates the P-incidence angle, the S-reflection angle, and the structural dip.

For the determination of the polarity flip in the angle domain we define θ_o as the *polarity flip angle*, for which the P-incidence angle equals the S-reflection angle and they are both equal to zero ($\beta_p = \beta_s = 0$), i.e normal incidence. Thus θ_o corresponds to the point of polarity flip in angle domain. Equation (8) reduces to:

$$\tan\theta_o = \tan\alpha \frac{v_p - v_s}{v_p + v_s} = \tan\alpha \frac{\gamma - 1}{\gamma + 1}. \tag{9}$$

It is important to emphasize that for constant γ the polarity flip will not necessarily occur at $\theta = 0$ because of the reflector dip effect.

Methodology

The polarity flip angle depends on both velocity fields and on the reflector's dip. Its determination is of crucial importance for the polarity regularization. This section describes the basic steps of our methodology for the polarity flip angle determination and polarity regularization. The algorithm that we use is:

1. Migrate common shot gathers to offset-domain CIGs.
2. Transform offset-domain gathers into angle-domain gathers (Sava and Fomel, 2000).
3. Determine the polarity flip angle, θ_o with equation (9).
4. Flip negative polarities in the angle domain.
5. Stack over angle to produce a final structural image.

The first step is to transform the data to the temporal frequency domain; subsequently, we downward continue the shot and receiver wavefields with v_p and v_s respectively, and image the data at zero time. In this way, we obtain the offset-domain CIGs, and if we use the correct velocity models, the energy is focused close to zero offset.

The common angle gathers are evaluated in the Fourier-domain by equation (10). The method involves a radial-trace mapping after migration in the k_h-k_z domain (Sava and Fomel, 2000). Rickett and Sava (2001) describe how we prepare the offset-domain CIGs with a shot-profile migration algorithm.

$$\tan\theta = -\frac{|\vec{k_h}|}{k_z}. \tag{10}$$

To determine the structural dip, we apply plane-wave destructors (Fomel, 2000), which characterize the seismic images as a superposition of local plane waves. With the dip field and the two migration velocity models, we calculate the polarity flip angle using equation (9). Flip the polarity is an easy process after we have the polarity flip angle: we just apply a mask to the common angle gathers that follows the polarity flip angles and multiply the data by -1.

NUMERICAL EXAMPLES

To test the methodology we created a realistic synthetic example. The model consists of four reflectors, dipping at angles of 15°, 0°, $-30°$, $-45°$, embedded in simple linear $v(z)$ velocities.

The velocity gradients were chosen in order to simulate a typical near seafloor velocity profile: the P-velocity model consists of an initial velocity of 1700 m/s and a gradient of 0.15 s^{-1}. On the other hand, the S-velocity model has an initial velocity of 300 m/s and a gradient of 0.35 s^{-1}.

We used ray-tracing in order to generate the data set. Figure 4 shows a common shot gather located in the center of the model. It is possible to note that the polarity flip varies with respect to the travel time as a function of the reflector dip and the $\frac{v_p}{v_s}$ ratio (Figure 2).

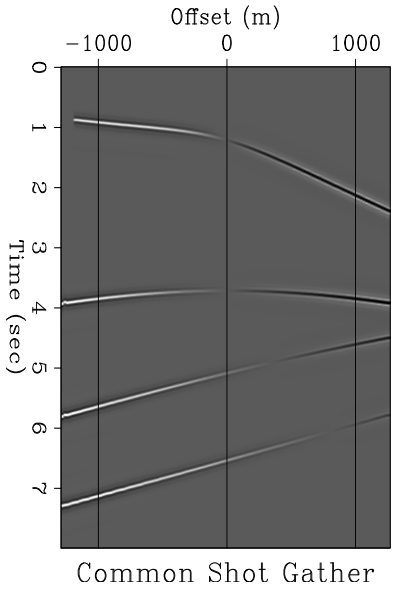

Figure 4: Common shot gather, taken in the middle of model. daniel2-csg2 [CR]

Figure 5 shows two angle-domain gathers after (left) and before (right) the polarity correction in the angle domain. The events in the common angle gathers are flat, this is not obvious for the $-45°$ event in the top of Figure 5, because of the low coverage in the modeling for that event at that depth. However, it is possible to observe that this event gets flatter with the rise in the fold, bottom of Figure 5. The flatness in the gathers implies that we used the correct velocity model for the migration. Moreover, it is possible to observe in the common angle gather before the correction that the same event changes its polarity. The point for this change is the polarity flip angle (θ_o) determined by equation (9). With the P and S velocity models used

for the migration and the dip map estimated by plane-wave destructors, we calculate the curve superimposed on the common angle gather, this curve represents the polarity flip angle. The angle-domain gather after the correction for the polarity inversion is in the right of Figure 5. It is clear that our methodology correctly handles the polarities after migration.

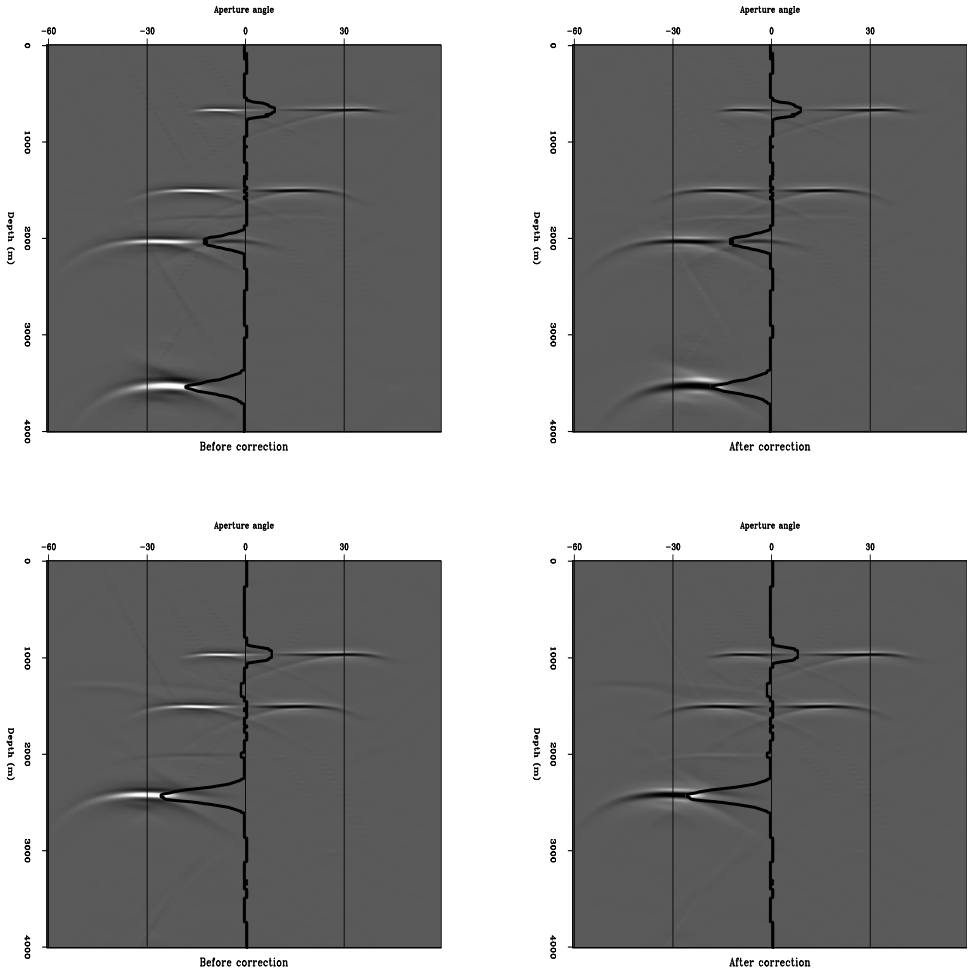

Figure 5: Two common angle gathers. After the prestack migration without the polarity correction (left). Before the prestack migration with the polarity correction (right). The line in the gathers mark the polarity flip angle, as a function of the dip, *P*-velocity and *S*-velocity. daniel2-cag2 [CR]

Figure 6 presents the final migration results. The top represents the result with the correction in the model space (flipping in the angle domain), the center represents the result with the correction in the data space (flipping the negative offsets), and the bottom represents the migration result without any correction. It is possible to observe that the correction in the model space perfectly recovered all the events with a strong illumination; the correction in the data space produced a weaker image for the dipping events; no correction resulted in the loss of the flat event.

CONCLUSIONS

We presented a series of important concepts in non-conventional PS-seismic processing for an important problem in converted wave seismic processing: the polarity flip.

We used frequency domain common shot migration in order to obtain an image of the subsurface with converted wave data. The shot-profile migration algorithm enables the use of two different velocity models, one for the P-wave path and the other for the S-wave path of the data; therefore, we do not have to introduce a mixed PS-velocity model.

We introduce common angle gather for converted waves. In this domain the normal incidence reflection is determined by the polarity flip angle, this polarity flip angle helps to regularize the polarities in the angle domain; we demonstrated this fact with a synthetic PS data set.

The introduction of common angle gather in converted waves seismic processing and imaging brings a series of opportunities for building S-velocity models, and analysis of amplitude versus angle for converted waves; therefore, the opportunity to extract as much information as possible from PS seismic data.

REFERENCES

Biondi, B., 2000, 3-D wave-equation prestack imaging under salt: 70th Ann. Internat. Mtg., Soc. Expl. Geophys., Expanded Abstracts, 906–909.

Claerbout, J. F., 1971, Toward a unified theory of reflector mapping: Geophysics, **36**, no. 3, 467–481.

Claerbout, J. F., 1985, Imaging the earth's interior: Blackwell Scientific Publications.

Danbom, S. H., and Domenico, S. N., 1988, Shear-wave exploration: Society of Exploration Geophysicists.

de Bruin, C. G. M., Wapenaar, C. P. A., and Berkhout, A. J., 1991, Angle-dependent reflectivity by means of prestack migration: Geophysics, **55**, no. 9, 1223–1234.

Fomel, S., 1996, Migration and velocity analysis by velocity continuation: SEP–**92**, 159–188.

Fomel, S., 2000, Applications of plane-wave destructor filters: SEP–**105**, 1–26.

Harrison, M. P., and Stewart, R. R., 1993, Poststack migration of P-SV seismic data: Geophysics, **58**, no. 8, 1127–1135.

Prucha, M., Biondi, B., and Symes, W., 1999, Angle-domain common image gathers by wave-equation migration: 69th Annual Internat. Mtg., Society Of Exploration Geophysicists, Expanded Abstracts, 824–827.

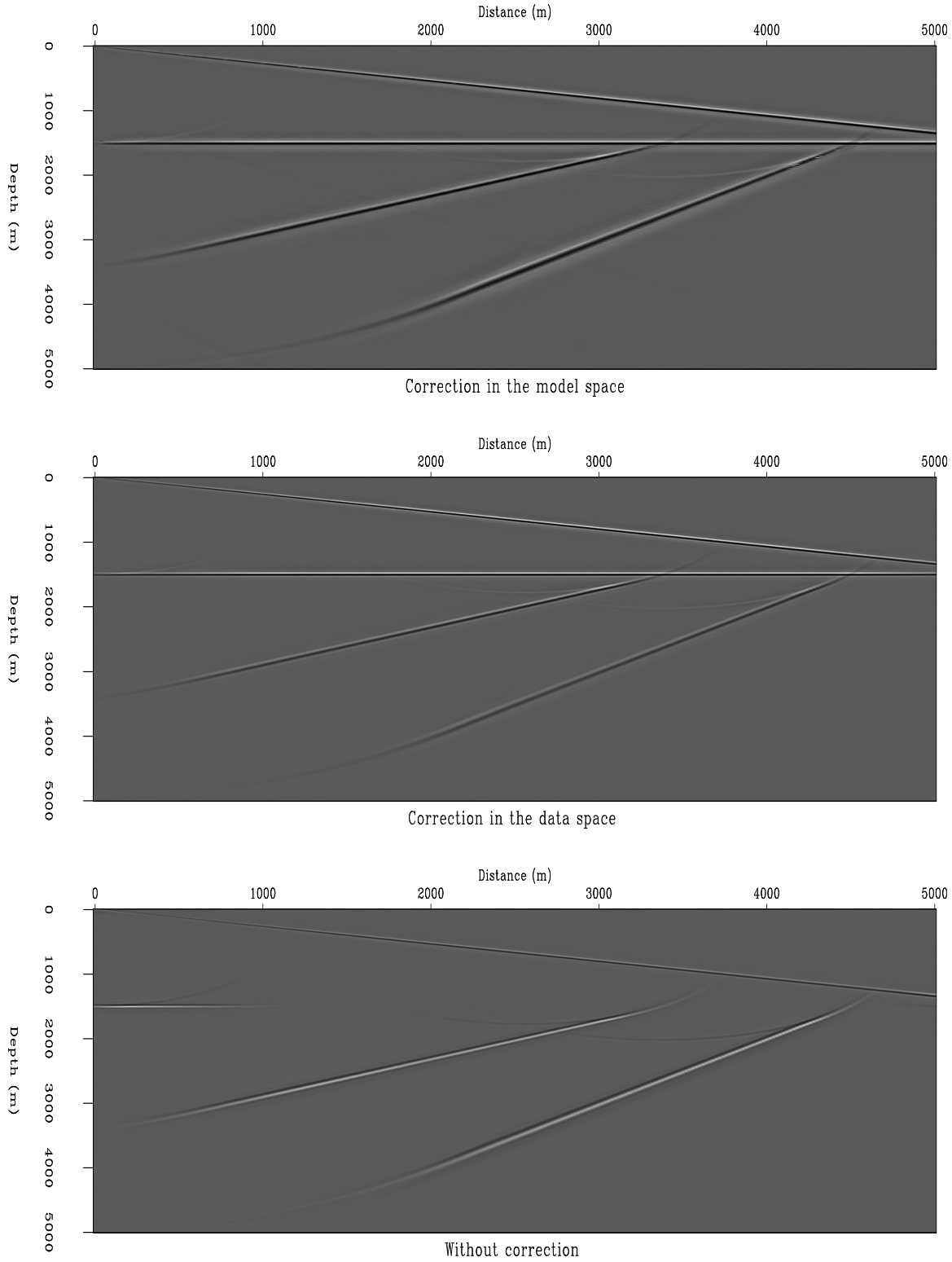

Figure 6: Final migration sections: The top figure shows the image with the polarity correction in the model space. The center figure shows the image with the polarity correction in the data space. The bottom figure shows the image without any correction daniel2-img2 [CR,M]

Rickett, J., and Sava, P., 2001, Offset and angle domain common image gathers for shot-profile migration: 71st Annual Internat. Mtg., Society Of Exploration Geophysicists, submitted.

Sava, P., and Fomel, S., 2000, Migration angle-gathers by Fourier Transform: Geophysical Prospecting, submitted.

Tatham, R. H., and McCormack, M. D., 1991, Multicomponent seismology in petroleum exploration: Society of Exploration Geophysicists.